Tuberculosis 89 (2009) 62–67

Contents lists available at ScienceDirect

Tuberculosis

journal homepage: http://intl.elsevierhealth.com/journals/tube

Protective efficacy of recombinant BCG Tokyo (Ag85A) in rhesus monkeys (*Macaca mulatta*) infected intratracheally with H37Rv *Mycobacterium tuberculosis*

I. Sugawara [a,*], L. Sun [b], S. Mizuno [a], T. Taniyama [c]

[a] *Mycobacterial Reference Center, The Research Institute of Tuberculosis, 3-1-24 Matsuyama, Kiyose, Tokyo 204-0022, Japan*
[b] *Animal Biosafety Level 3 Laboratory, The Center for Animal Experimentation, Wuhan University, Wuhan, China*
[c] *National Institute for Infectious Diseases, Tokyo 162-8640, Japan*

ARTICLE INFO

Article history:
Received 24 March 2008
Received in revised form
3 September 2008
Accepted 24 September 2008

Keywords:
Mycobacterium tuberculosis H37Rv
Ag85A
Recombinant BCG
Rhesus monkey

SUMMARY

We have reported previously that recombinant BCG Tokyo (Ag85A) (rBCG-Ag85A[Tokyo]) shows promise as a tuberculosis vaccine, demonstrating protective efficacy in cynomolgus monkeys. As a next step, rhesus monkeys were utilized because they are also susceptible to *Mycobacterium tuberculosis* and show a continuous course of infection resembling human tuberculosis. The recombinant BCG vaccine (5×10^5 CFU per monkey) was administered once intradermally into the back skin to three groups of rhesus monkeys, and its protective efficacy was compared for 4 months with that of its parental BCG Tokyo strain. Eight week vaccination of the monkeys with rBCG-Ag85A[Tokyo] resulted in a reduction of tubercle bacilli CFU ($p < 0.01$) and lung pathology in animals infected intratracheally with 3000 CFU H37Rv *M. tuberculosis*. Vaccination prevented an increase in the old tuberculin test after challenge with *M. tuberculosis* and reaction of *M. tuberculosis*-derived antigen. Thus, it was shown that even in rhesus monkeys rBCG-Ag85A[Tokyo] induced higher protective efficacy than BCG Tokyo.

1. Introduction

Tuberculosis (TB) still remains a major health problem affecting millions of people worldwide. The only TB live attenuated vaccine currently available is *Mycobacterium bovis* BCG. However, the efficacy of BCG against adult pulmonary tuberculosis still remains controversial.[1–4] Thus, development of a better TB vaccine is urgently required in order to counteract the global threat of TB.

Several TB vaccines are currently being tested using various models[5–9] and several recent reviews have been published.[10–13] These include recombinant BCG vaccine expressing Ag85B, recombinant modified vaccinia virus Ankara expressing Ag85A, TB polyprotein vaccine, Mtb72f, ESAT-6 subunit vaccine, auxotrophic vaccines for TB, and recombinant BCG overexpressing major extracellular proteins (rBCG30). Although there have been few reports on the efficacy of TB vaccine candidates in cynomolgus monkey models due to the lower availability of monkey P3 facilities, a few papers have described the use of primate models. Vaccination of cynomolgus monkeys with Ag85B-ESAT-6 reportedly induces protective immune responses.[14] DNA vaccine (HSP65 + IL-12/HVJ) as well as 72f recombinant BCG provide better protective efficacy in cynomolgus monkeys.[15]

We have previously reported the protective efficacy of a TB DNA vaccine (Ag85A) and a recombinant strain BCG Tokyo (Ag85A) in small-animal models challenged with *M. tuberculosis* Kurono strain.[16,17] We found that recombinant BCG Tokyo was better than Ag85A DNA in terms of protective efficacy against *M. tuberculosis*.[6] The spleen tissues from guinea pigs vaccinated with rBCG-Ag85A[Tokyo] or Ag85A DNA expressed IFN-γ and IL-2 mRNA at significantly high levels.[6] This finding prompted us to explore further the efficacy of rBCG-Ag85A[Tokyo] in cynomolgus monkeys.[18] We chose cynomolgus monkeys because this animal is reportedly protected more efficiently than rhesus monkeys by BCG vaccination.[19] Previous studies have shown that whereas the rhesus macaque is highly susceptible to *M. tuberculosis*, the closely related cynomolgus macaque is more resistant.[20–22] Thus, we thought that cynomolgus monkeys would be more efficiently protected by BCG vaccination than rhesus monkeys and therefore afford a good experimental model for the evaluation of new TB vaccine candidates. When we used cynomolgus monkeys, we found that rBCG-Ag85A[Tokyo] induced higher protective efficacy than the parental BCG Tokyo.[18]

There are still pros and cons for the experimental use of rhesus monkeys using BCG TB vaccines.[19,21,23,24] Barclay et al. have reported that a high level of resistance to infection could be induced by BCG vaccine in the rhesus monkey, which in nature is highly

* Corresponding author. Tel.: +81 42 493 5075; fax: +81 42 492 4600.
E-mail address: sugawara@jata.or.jp (I. Sugawara).

1472-9792/$ – see front matter © 2008 Elsevier Ltd. All rights reserved.
doi:10.1016/j.tube.2008.09.008

susceptible to tuberculous infection. Janicki et al. have demonstrated high immune responses in rhesus monkeys after bacillus Calmette–Guerin vaccination and aerosol challenge with *M. tuberculosis*. However, Langermans' observation that BCG does not substantially protect rhesus monkeys from pulmonary *M. tuberculosis* infection contradicts earlier studies. It may be due to the higher *M. tuberculosis* challenge dose that he used to allow a direct comparison between cynomolgus and rhesus monkeys. There are few reports of the use of TB vaccines in rhesus monkeys.[25,26] However, it is worth using rhesus monkeys in TB vaccination studies because cynomolgus and rhesus monkeys are closely related phylogenetically. As a next step, therefore, rhesus monkeys were utilized to see whether or not this rBCG-Ag85A[Tokyo] has promise as a TB vaccine. Even in cynomolgus monkeys, this vaccine induced higher protective efficacy than BCG Tokyo.

2. Materials and methods

2.1. Construction of recombinant (r)BCG Tokyo (rBCG-Ag85A[Tokyo])

rBCG-Ag85A[Tokyo] was constructed as described previously.[18] Briefly, the Ag85A gene was amplified by PCR and subcloned into the pCR4 vector. The presence of the Ag85A gene was then confirmed by DNA sequencing. The gene was inserted into the pBBN vector (Ag85A-HA) possessing a hemagglutinin (HA) tag at its 5′ end. At this stage, the Ag85A-HA was expressed in *E. coli*, and then the Ag85A-HA gene was introduced into the downstream region of the pHPS integration vector. The vector was then electroporated into BCG Tokyo. The resulting transformants (rBCG-Ag85A[Tokyo]) were cultured individually and the content of the extracted lysate that contains Ag85 protein was confirmed by Western blotting.[17]

2.2. Bacterial strain

Mycobacterium tuberculosis H37Rv (ATCC 25618) was passed through mice and grown once in 7H9 liquid medium before titration and storage in aliquots at −85 °C. The culture strain was filtered through a membrane filter (4-μm pore size; Millipore, Bedford, MA, USA) before use to ensure even dispersal.

2.3. Monkeys

A total of 15 rhesus male monkeys (*Macaca mulatta*) (8–9 kg, 6–8 years old) were used. They were purchased from Laboratory Animal Center, Academy of Military Medical Sciences, Beijing, China. All animals were housed at the animal biosafety level (ABSL) 3 facility of Wuhan University, Wuhan, China. The animals were studied in groups of three. Before the start of the studies, all animals were examined clinically and radiologically, and tuberculin skin-tested. For intratracheal challenge, animals were anesthetized with ketamine. Prior to commencement, the experiments were reviewed and approved by the Wuhan University ethics committee. We used a ketamine anesthetic for euthanasia.

2.4. Inoculation of monkeys

The monkeys were randomly assigned to three groups. Group 1 (three monkeys) received one intradermal injection of 5×10^5 CFU/ml rBCG-Ag85A[Tokyo]. Group 2 (three monkeys) received one intradermal injection of 5×10^5 CFU/ml BCG Tokyo. BCG Tokyo was kindly supplied by Dr. S. Yamamoto. Group 3 comprised of three unvaccinated monkeys that received physiological saline as a control.

The other six monkeys in three groups were followed up for 10 months to investigate long-term survival after vaccination and subsequent infection with H37Rv.

2.5. Intratracheal infection of monkeys

Eight weeks after vaccination, the animals were challenged by intratracheal instillation of 1 ml (3000 CFU) of H37Rv *M. tuberculosis*. All animals were challenged on the same day with the same preparation, and were then observed for 4 months after infection. As PPD (0.5 μg/ml) did not give better positive results for the monkeys, old tuberculin was used. The old tuberculin test (Chemo-Sero-Therapeutic Research Institute, Kumamoto, Japan) was carried out 1, 2 and 3 months after infection.[18] Briefly, 0.1 ml of old tuberculin solution was injected intradermally into the left palpebral skin and 0.1 ml saline was injected intradermally into the right palpebral skin. Two days later, swelling and redness on both sides were compared and the diameter of redness was measured. All animals were housed in animal biosafety level (ABSL) 3 facilities.

2.6. Animal care

After infection, animals were observed daily by the animal caretakers for changes in behavior, eating and coughing. Weight, erythrocyte sedimentation rate (ESR) and temperature were recorded at times of blood sampling. Body temperature was measured rectally.

2.7. Immunological examination

Blood from the femoral vein was used to obtain serum. TB Dot assay (Shanghai Upper Biotech and Pharma Co., Shanghai, China) was carried out in accordance with the instruction sheet provided by the manufacturer to evaluate *M. tuberculosis* infection.[18] This Dot assay detects 38 kDa antigen derived from *M. tuberculosis*.[18]

2.8. Bacterial enumeration

For the unvaccinated monkeys, 10 samples from the upper and lower lobes of the lung, and also spleen tissue, about 0.5 cm^3 in size were taken randomly at necropsy. For the vaccinated monkeys, 10 similar samples were taken randomly at necropsy. After being weighed, the samples were combined, homogenized and serially diluted with physiological saline. For the vaccinated groups, pyrazinamide (200 μg/20 μl) was added to determine BCG Tokyo-derived colonies (background count). To examine *M. tuberculosis*-derived colonies, the background count was subtracted from the number of colonies.[18] The lung and spleen tissues were weighed and the results were expressed as CFU ± SD/g organ.

2.9. Histopathology

As soon as the unvaccinated monkeys died, they were frozen immediately in a deep freezer. Necropsies were undertaken on the same day for the unvaccinated frozen monkeys and the vaccinated monkeys after euthanasia. The removed organs were fixed with 15% formalin for 10 days. Tissue sections from paraffin blocks containing lung, spleen, hilar lymph nodes and liver were stained with hematoxylin and eosin or the Ziehl–Neelsen method for acid-fast bacilli. The severity of pulmonary lesions was judged independently by two experts in a blind manner (I.S. and S.M.).

2.10. Statistical analysis

We performed analysis of variance (ANOVA) for repeated measurements using the baseline results at screening as a covariate on log-transformed data to compare between groups.

3. Results

3.1. Clinical course

The rhesus monkeys vaccinated with rBCG-Ag85A[Tokyo] or parental BCG Tokyo and their non-vaccinated controls were infected intratracheally with H37Rv *M. tuberculosis*. Three rBCG-Ag85A[Tokyo]-vaccinated monkeys and two BCG Tokyo-vaccinated monkeys survived until the time of necropsy. Furthermore, when we followed up the rBCG-Ag85A[Tokyo]-vaccinated and BCG Tokyo-vaccinated monkeys (two/experimental group) for 10 months, only vaccinated monkeys survived till the time of necropsy. No coughing was observed in the animals after challenge. None of the vaccinated animals gained weight during the infection period. Their ESR was within the normal range (1–2 mm/h). None of the non-vaccinated animals showed an appreciable increase in body weight. Two of the monkeys (4 and 5) showed a gradual decrease in weight (50 g). The three non-vaccinated control animals showed a severe decrease in weight of 500–1000 g, and their ESR was higher than the reference value (18, 35 and 40 mm/h) (Table 1).

On radiographs of the chest, the non-vaccinated animals exhibited early development of multilobar pneumonia in the right lung and rapid progression to bilateral pneumonia. Lobar consolidation and atelectasis in the involved lungs and hilar lymphadenopathy were observed frequently in the non-vaccinated groups (Table 1).

In the vaccinated groups, pneumonia was slight to mild (Figure 1).

3.2. Immunological responses

Two immunological methods (the old tuberculin test and serum tuberculosis diagnosis) were utilized to clarify the severity of *M. tuberculosis* infection. In the vaccinated monkeys two months after infection, the old tuberculin test gave a positive result. In the non-vaccinated animals 1 day before death, the reaction was strongly positive and marked palpebral reddish skin swelling was observed and the sizes of redness were measured (Table 1).

The TB dot assay gave a negative result in all vaccinated and non-vaccinated animals 1 month after infection. However, 2 months after infection, the result was positive in the vaccinated monkeys, and strongly positive (2+) in the non-vaccinated monkeys (data not shown).

Table 1
Summary of the rhesus monkey experiments.

Monkey No.	Vaccination	Lung histopathology	ESR (mm/h, 2 months)	Sizes of old tuberculin (mm, 1 month)	Chest X-ray before death or necropsy
1	Rec BCG	Pneumonia Granulomas	2	13	Pneumonia
2	Rec BCG	Pneumonia	2	17	Pneumonia
3	Rec BCG	Pneumonia	2	12	Pneumonia
4	BCG Tokyo	Pneumonia Granulomas	2	15	Pneumonia
5	BCG Tokyo	Pneumonia Granulomas	1	18	Pneumonia
6	BCG Tokyo	Pneumonia	2	15	Pneumonia
7	Saline	Granulomas	35	31	Consolidation Pneumonia
8	Saline	Granulomas	18	28	Consolidation Pneumonia
9	Saline	Granulomas	40	37	Consolidation Pneumonia

Rec BCG; recombinant BCG.

3.3. Gross pathology and histopathology of the vaccinated and non-vaccinated monkeys

At necropsy, all unvaccinated animals showed extensive bilateral lung pathology characterized by the presence of multiple granulomas. These granulomas showed conglomeration to larger caseous areas, especially in the hilar region. Granulomas were also present in the liver and spleen. In the vaccinated animals, a few small granulomas were evident, but these showed no caseous changes. Small liver granulomas were not observed in the recombinant BCG-vaccinated monkeys, but were evident in BCG-vaccinated monkeys. One BCG-vaccinated monkey died after 59 days after infection, but the cause of death was not due to advanced tuberculosis at necropsy. Three non-vaccinated monkeys died of advanced tuberculosis 46, 49 and 58 days after infection. These were frozen just after death and necropsied for further examination.

On microscopic examination, the non-vaccinated animals showed multifocal, coalescing granulomas with central necrosis and pronounced cellular infiltrates in the periphery (Figure 2). The vaccinated animals showed markedly less severe histopathology. In particular, the peripheral inflammatory cell infiltration suggesting severe pneumonia was notably more pronounced in the unvaccinated than in the vaccinated animals. No multinucleated giant cells were recognized in the granulomas. Histological examination of the three animals that had received the recombinant BCG (Ag85A) showed almost normal lung tissue without granulomas in two of them. The remaining vaccinated animal showed a solitary small granuloma without central necrosis. Two BCG Tokyo-vaccinated animals showed a single small granuloma (Table 1). One BCG Tokyo-vaccinated monkey died 59 days after infection, but the cause of death was not due to advanced tuberculosis as evaluated by histological examination.

3.4. Replication of tubercle bacilli in the lung and spleen tissues of vaccinated and non-vaccinated monkeys

At autopsy, 10 different samples of lung and spleen tissue were taken for determination of CFU. Background culture CFU of BCG Tokyo or rBCG-Ag85A[Tokyo] after addition of pyrazinamide to the tissue homogenates was one or two. The lung tissue of animals vaccinated with recombinant BCG showed a significant 10-fold decrease in the number of bacteria compared with the non-vaccinated animals ($p < 0.01$). The number of CFU in BCG Tokyo-vaccinated animals after 16 weeks of infection was reduced 10-fold relative to that in the non-vaccinated animals ($p < 0.01$). There was a statistically significant difference in the number of pulmonary CFU between recombinant BCG-vaccinated and BCG Tokyo-vaccinated animals ($p < 0.01$) (Figure 3).

A similar tendency was also observed in the number of splenic CFU. The spleen tissues of animals vaccinated with recombinant BCG or BCG Tokyo showed a significant 100-fold or 10-fold decrease in the number of bacteria compared with the non-vaccinated animals ($p < 0.01$). There was also a statistically significant difference in the number of splenic CFU between recombinant BCG-vaccinated and BCG-vaccinated animals ($p < 0.01$).

4. Discussion

Although there are advantages and drawbacks to the use of rhesus monkeys for evaluation of TB vaccines, we have demonstrated that vaccination of rhesus monkeys with recombinant BCG (Ag85A) (rBCG-Ag85A[Tokyo]) induces protection against intratracheal infection with H37Rv *M. tuberculosis*. In addition to measurement of protection in terms of reduction of bacterial number and/or lung pathology, we have also shown that

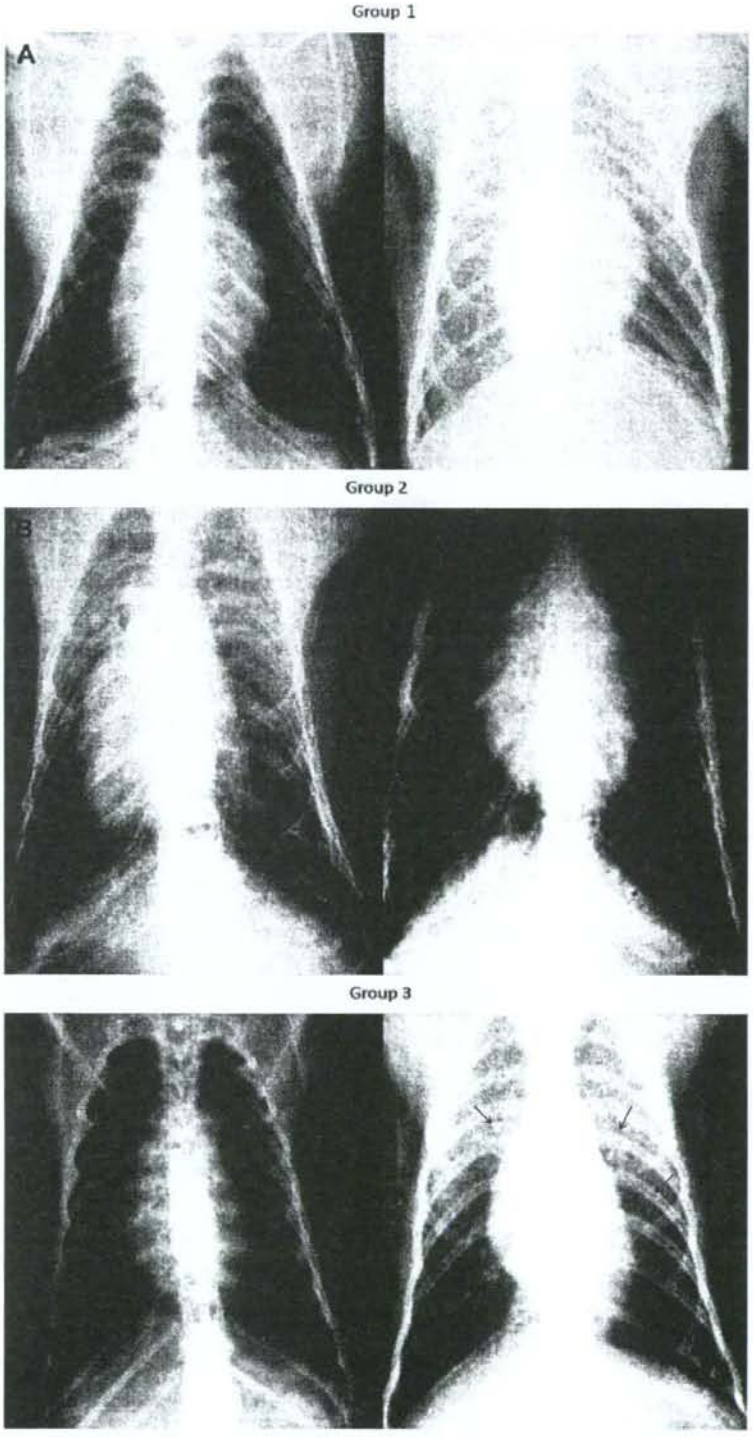

Figure 1. Chest radiologic examinations after challenge with H37Rv *M. tuberculosis*. (A) Rhesus monkey (No. 3) vaccinated with rBCG-Ag85A[Tokyo]. Left, before infection. Right, after infection. The chest X-ray picture (right) was taken 1 day before necropsy. (B) Monkey (No. 6) vaccinated with parental BCG Tokyo. Left, before infection. Right, after infection. The chest X-ray picture (right) was taken 1 day before necropsy. (C) Non-vaccinated monkey (No. 8) 2 days before death (right). Left, before infection. Right, after infection. After H37Rv challenge, the non-vaccinated monkeys rapidly developed extensive bronchopneumonia. Many nodular shadows (→) were recognized, but the vaccinated monkeys had negative chest X-ray findings 3 months after H37Rv challenge.

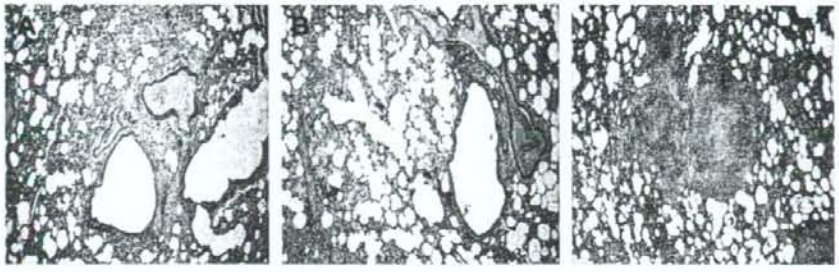

Figure 2. Histopathology of lung tissues from *M. tuberculosis*-infected rhesus monkeys vaccinated with rBCG-Ag85A[Tokyo] (A), BCG Tokyo (B) or non-vaccinated control which died 58 days after intratracheal infection (C) at necropsy. The granuloma with caseating necrosis are surrounded peripherally by a dense infiltrate of epithelioid macrophages and lymphocytes (C), but in the vaccinated monkeys interstitial pneumonia is evident (A and B). ×20. Hematoxylin and eosin stain.

recombinant BCG vaccination prevented the development of a number of important clinical and immunological changes during infection. These changes included an increase of the ESR and the development of strong immune responses to a wide spectrum of mycobacterial antigens (old tuberculin). When we inoculated monkeys once with 5×10^5 CFU rBCG-Ag85A[Tokyo], there was a significant reduction of CFU in lung and spleen tissues compared to that in BCG Tokyo-inoculated monkeys.

When parental BCG Tokyo was used for vaccination, we found several grayish tubercles in the liver in two of six monkeys, but no such tubercles were evident in monkeys vaccinated with recombinant BCG. Moreover, there was a significantly lower number of CFU in lung tissues of monkeys vaccinated with recombinant BCG than in monkeys vaccinated with BCG Tokyo ($p < 0.01$). Taken together, the results suggest that the recombinant BCG bearing the introduced Ag85A gene gives better protective efficacy than BCG Tokyo. In order to evaluate the efficacy of the Ag85A antigen carefully, it was necessary to lower the dose of recombinant BCG. This time we used 5×10^5 CFU, which was one fourth of the dose used for cynomolgus monkeys. Again, rBCG-Ag85A[Tokyo] was effective in protecting against rhesus monkey tuberculosis.

In cynomolgus monkey experiments, many small nodules (macroscopically yellowish nodules) were seen throughout the entire lungs, indicating the presence of miliary tuberculosis. However, in rhesus monkeys, pulmonary consolidation with larger nodules was a major feature. It is suggested that rhesus monkeys are more susceptible to *M. tuberculosis* than cynomolgus monkeys. We carefully examined the lung histopathology of the vaccinated and non-vaccinated rhesus monkeys, but no multinucleated giant cells were observed. This is in sharp contrast to the previously reported study.[19] We have examined granulomas of mice, rats and guinea pigs infected with *M. tuberculosis*, but did not observe multinucleated giant cells except in IFN-γ-deficient mice infected with BCG Pasteur.[27] Although IFN-γ plays an essential role in formation of multinucleated giant cells, its exact role remains unknown.

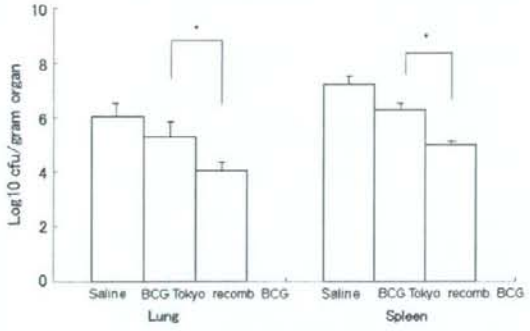

Figure 3. CFU counts in lung and spleen tissues per gram of H37Rv *M. tuberculosis*-infected rhesus monkeys vaccinated with BCG Tokyo or recombinant BCG Tokyo (Ag85A), and in non-vaccinated controls. * significant difference at $p < 0.01$.

The TB dot assay, which targets the 38 kDa antigen from *M. tuberculosis*, gave a negative result 1 month after infection, but a positive one 2 months after infection in rhesus monkey as well as cynomolgus monkey experiments. Therefore, care is needed when diagnosing tuberculosis in the early phase. The old tuberculin test may be more useful for diagnosis of early-phase TB. We were able to measure Ag85 antigen in sera of the rBCG-Ag85A[Tokyo]-vaccinated monkeys by ELISA (data not shown).

We selected Ag85A as a promising immunogen because the protein from *M. tuberculosis* induces significant humoral and cell-mediated immune responses.[28,29] The expression levels of IFN-γ and IL-2 mRNAs were increased in spleen tissues from guinea pigs that had been vaccinated with parental BCG Tokyo, recombinant (r)BCG-Ag85A[Tokyo], and Ag85A DNA vaccine. Among them, the expression levels of IFN-γ and IL-2 mRNAs were the highest after vaccination with rBCG-Ag85A[Tokyo].[17] Furthermore, the sera from the rBCG-Ag85A[Tokyo]-vaccinated guinea pigs were significantly reactive with the Ag85A peptide we used in our previous study (data not shown). We have shown previously that vaccination with Ag85A DNA twice by gene gun bombardment or with rBCG-Ag85A[Tokyo] once significantly reduced the severity of pulmonary pathology and the number of CFU in guinea pigs.[16,17] When the immunogenic synthetic Ag85A peptide was further used as a booster together with recombinant BCG (Ag85A), lung pathology was improved significantly, together with a significant reduction in the number of pulmonary CFU.[17] Although a single intradermal inoculation of 5×10^5 CFU BCG (Ag85A) was enough to induce protective efficacy in the present study, it would be desirable to use Ag85A peptide as a booster, Ag85B-ESAT-6 fusion protein and 72f fusion protein in combination with recombinant BCG Tokyo (Ag85A) to achieve much better protective efficacy.[8,17]

Several promising TB vaccine candidates are now available after verification in monkey experiments. We plan to perform a global multicenter study of the TB vaccine thus chosen using the same experimental protocols after TB vaccine researchers have evaluated their TB vaccines and selected a promising one on the basis of consensus.

In summary, we have shown in a series of primate experiments that vaccination of primates (rhesus and cynomolgus monkeys) with rBCG-Ag85A[Tokyo] induces good protective immune responses. Using the rhesus monkey challenge model, further optimization of the dose should yield levels of protection that are better than those achieved with recombinant BCG.

Acknowledgements

Part of this study was supported by a grant for emerging and reemerging infectious diseases supported by the Ministry of Health, Labor and Welfare, Japan (PI: Dr. Masaji Okada). We would like to thank Mr. Qiaoyan Xian and other laboratory staff at Wuhan University for their help and cooperation. Part of this work was presented at the 43rd US–Japan CMSP Tuberculosis and Leprosy Research Conference in Baltimore, US, in 2008.

Funding: Please see Acknowledgements.

Competing interests: None declared.

Ethical approval: Not required.

References

1. Clemens JD, Chuong JJ, Feinstein AR. The BCG controversy. A methodological and statistical reappraisal. *JAMA* 1983;**249**:2362–9.
2. Zodpey SP. The BCG controversy: a reappraisal of the protective effect against tuberculosis and leprosy. *Indian J Public Health* 2004;**48**:70–7.
3. Haile M, Kallenius G. Recent developments in tuberculosis vaccines. *Curr Opin Infect Dis* 2005;**18**:211–5.
4. Andersen P, Doherty TM. The success and failure of BCG: implications for a novel tuberculosis vaccine. *Nat Rev Microbiol* 2005;**3**:656–62.
5. Chambers MA, Williamas A, Hatch G, Gavier-Widen D, Hall G, Huygen K, et al. Vaccination of guinea pigs with DNA encoding the mycobacterial antigen MPB83 influences pulmonary pathology but not hematogenous spread following aerogenic infection with *Mycobacterium bovis*. *Infect Immun* 2002;**70**:2159–65.
6. Horwitz MA, Harth G, Dillon BJ, Maslesa-Galic S. Recombinant bacillus Calmette–Guerin (BCG) vaccines expressing the *Mycobacterium tuberculosis* 30-kDa major secretory protein induce greater protective immunity against tuberculosis than conventional BCG vaccines in a highly susceptible animal model. *Proc Natl Acad Sci USA* 2000;**97**:13853–8.
7. Skeiky YAW, Alderson MR, Ovendale PJ, Guderian JA, Brandt L, Dillon DC, et al. Differential immune responses and protective efficacy induced by components of a tuberculosis polyprotein vaccine, Mtb72F, delivered as naked DNA or recombinant protein. *J Immunol* 2004;**172**:7618–28.
8. Brandt L, Skeiky YA, Alderson MR, Lobet Y, Dalemans W, Turner OC, et al. The protective effect of the *Mycobacterium bovis* BCG vaccine is increased by coadministration with the *Mycobacterium tuberculosis* 72-kilodalton fusion polyprotein Mtb72F in *M. tuberculosis*-infected guinea pigs. *Infect Immun* 2004;**72**:6622–32.
9. Guleria I, Teitelbaum R, McAdams RA, Kaplan G, Jacobs Jr WR, Bloom BR. Auxotrophic vaccines for tuberculosis. *Nat Med* 1996;**2**:334–7.
10. Reed S, Lobet Y. Tuberculosis vaccine development: from mouse to man. *Microbes Infect* 2005;**7**:922–31.
11. Dietrich J, Lundberg CV, Andersen P. TB vaccine strategies—what is needed to solve a complex problem? *Tuberculosis* 2006;**86**:163–8.
12. Skeiky YA, Sadoff JC. Advances in tuberculosis vaccine strategies. *Nat Rev Microbiol* 2006;**4**:469–76.
13. Kaufmann SH, Baumann S, Nasser Eddine A. Exploiting immunology and molecular genetics for rational vaccine design against tuberculosis. *Int J Tuberc Lung Dis* 2006;**10**:1068–79.
14. Langermans JAM, Doherty TM, Vervenne RAW, van der Laan T, Lyashchenko K, Greenwald R, et al. Protection of macaques against *Mycobacterium tuberculosis* infection by a subunit vaccine based on a fusion protein of antigen 85B and ESAT-6. *Vaccine* 2005;**23**:2740–50.
15. Kita Y, Tanaka T, Yoshida S, Ohara N, Kaneda Y, Kuwayama S, et al. Novel recombinant BCG and DNA-vaccination against tuberculosis in a cynomolgus monkey model. *Vaccine* 2005;**23**:2132–5.
16. Sugawara I, Yamada H, Udarawa T, Huygen K. Vaccination of guinea pigs with DNA encoding Ag85A by gene gun bombardment. *Tuberculosis* 2003;**83**:331–7.
17. Sugawara I, Udagawa T, Taniyama T. Protective efficacy of recombinant (Ag85A) BCG Tokyo with Ag85A peptide boosting against *Mycobacterium tuberculosis*-infected guinea pigs in comparison with that of DNA vaccine encoding Ag85A. *Tuberculosis* 2007;**87**:94–101.
18. Sugawara I, Li Z, Sun L, Udagawa T, Taniyama T. Recombinant BCG Tokyo (Ag85A) protects cynomolgus monkeys (*Macaca fascicularis*) infected with H37Rv *Mycobacterium tuberculosis*. *Tuberculosis* 2007;**87**:518–25.
19. Langermans JA, Andersen P, van Soolingen D, Vervenne RA, Frost PA, vander Laan T, et al. Divergent effect of bacillus Calmette–Guerin (BCG) vaccination on *Mycobacterium tuberculosis* infection in highly related macaque species: implications for primate models in tuberculosis vaccine research. *Proc Natl Acad Sci USA* 2001;**98**:11497–502.
20. Good RC. Biology of the mycobacterioses Simian tuberculosis: immunologic aspects. *Ann NY Acad Sci* 1968;**154**:200–13.
21. Ribi E, Anacker RL, Barclay WR, Brehmer W, Harris SC, Leif WR, et al. Efficacy of mycobacterial cell walls as a vaccine against airborne tuberculosis in the Rhesus monkey. *J Infect Dis* 1971;**123**:527–38.
22. Walsh GP, Tan EV, dela Cruz EC, Abalos RM, Villahermosa LG, Young LJ, et al. The Philippine cynomolgus monkey (*Macaca fascicularis*) provides a new nonhuman primate model of tuberculosis that resembles human disease. *Nat Med* 1996;**2**:430–6.
23. Barclay WR, Anacker RL, Brehmer W, Leif W, Ribi E. Aerosol-induced tuberculosis in subhuman primates and the course of the disease after intravenous BCG vaccination. *Infect Immun* 1970;**2**:574–82.
24. Janicki BW, Good RC, Minden P, Affronti LF, Hymes WF. Immune responses in rhesus monkeys after bacillus Calmete–Guerin vaccination and aerosol challenge with *Mycobacterium tuberculosis*. *Am Rev Respir Dis* 1973;**107**:359–66.
25. Gormus BJ, Baskin GB, Xu K, Bohm RP, Mack PA, Ratterree MS, et al. Protective immunization of monkeys with BCG or BCG plus heat-killed *Mycobacterium leprae*: clinical results. *Lepr Rev* 1998;**69**:6–23.
26. Attanasio R, Pehler K, McClure HM. Immunogenicity and safety of *Mycobacterium tuberculosis* culture filtrate proteins in non-human primates. *Clin Exp Immunol* 2000;**119**:84–91.
27. Sugawara I, Yamada H, Kazumi Y, Doi N, Otomo K, Aoki T, et al. Induction of granulomas in IFN-gamma gene-disrupted mice by avirulent but not by virulent strains of *Mycobacterium tuberculosis*. *J Med Microbiol* 1998;**47**:871–7.
28. Kamath AT, Feng CG, MacDonald M, Briscoe H, Britton WJ. Differential protective efficacy of DNA vaccines expressing secreted proteins of *Mycobacterium tuberculosis*. *Infect Immun* 1999;**67**:1702–7.
29. Huygen K, Content J, Denis O, Montgomery DL, Yawman AM, Deck RR, et al. Immunogenicity and protective efficacy of a tuberculosis DNA vaccine. *Nat Med* 1996;**2**:893–8.

Tohoku J. Exp. Med., 2008, **216**, 363-370

Higher Susceptibility of Type 1 Diabetic Rats to *Mycobacterium tuberculosis* Infection

ISAMU SUGAWARA[1] and SATORU MIZUNO[1]

[1]Mycobacterial Reference Center, The Research Institute of Tuberculosis, Japan Anti-Tuberculosis Association, Tokyo, Japan

An association between diabetes mellitus and tuberculosis has been implicated for a long time. We have previously reported that Goto Kakizaki type 2 diabetic rats are highly susceptible to *Mycobacterium (M.) tuberculosis* infection. As a next step, we attempted to clarify whether type 1 diabetic rats are more susceptible to *M. tuberculosis* than non-diabetic wild-type (WT) rats. Here, we used the Komeda diabetes-prone (KDP) rat, as a model of type 1 diabetes mellitus. The infected KDP rats developed large granulomas without central necrosis in their lungs, liver or spleen. This was consistent with a significant increase in the number of colony-forming units (cfu) of *M. tuberculosis* in the lungs and spleen ($p < 0.01$). Insulin treatment resulted in significant reduction of tubercle bacilli in the infected KDP rats ($p < 0.01$). Pulmonary levels of interferon-γ, tumor necrosis factor-α and interleukin-1β mRNAs were higher in the infected diabetic rats than in WT rats. Alveolar macrophages from KDP rats were not fully activated by *M. tuberculosis* infection because the macrophages did not secrete nitric oxide (NO) that can kill *M. tuberculosis* ($p < 0.01$), but no significant difference in phagocytosis of tubercle bacilli by alveolar macrophages was observed between KDP and WT rats. Taken together, our findings indicate that type 1 diabetic rats are more susceptible to *M. tuberculosis* that WT rats.

——— type 1 diabetic rat; type 1 diabetes mellitus; tuberculosis; cytokine.

Tohoku J. Exp. Med., 2008, **216** (4), 363-370.

Patients with diabetes mellitus (DM) seem to be at high risk of developing tuberculosis, and DM is one of the risk factors for tuberculosis. It has been implicated that there is a clinical link between diabetes mellitus and pulmonary tuberculosis (Garay 2004), and several studies have investigated this issue (Banyai 1931; Root 1934; Boucot et al. 1952; Kim et al. 1995). As patients with DM are increasing worldwide, it is important to examine why diabetic patients are susceptible to *M. tuberculosis* infection.

DM is broadly classified into two types: type 1 (insulin-dependent) and type 2 (insulin-independent) (Powers 2008). There are several animal models of DM including non-obese diabetic (NOD) mice and spontaneously diabetic Goto Kakizaki (GK) rats (Goto et al. 1976; Makino et al. 1976). When GK rats were used to examine the relationship between type 2 DM and tuberculosis, we found that the rats developed large granulomas and that their alveolar macrophages were not fully activated by *Mycobacterium (M.) tuberculosis* infection (Sugawara et al. 2004). This was consistent with the significantly increased

Received August 21, 2008; revision accepted for publication November 11, 2008.

Correspondence: Dr. Isamu Sugawara, Mycobacterial Reference Center, The Research Institute of Tuberculosis, 3-1-24 Matsuyama, Kiyose, Tokyo 204-0022, Japan.

e-mail: sugawara@jata.or.jp

number of colony-forming units of *M. tuberculosis* in the lung and spleen tissues.

We then examined the relationship between type 1 DM and experimental tuberculosis. As at the time there was no rat model of type 1 diabetes, NOD type 1 mice were utilized instead for this purpose. The results were variable and inconsistent. NOD mice developed large granulomas in one experiment, but not in another experiment. It has been reported previously that NOD mice are resistant to *M. avium* and that the infection prevents autoimmune disease (Bras and Aguas 1996). Moreover, protection of NOD mice from diabetes is a Th1-type response that is mediated by up-regulation of the Fas-FasL pathway and involves an increase in the cytotoxicity of T cells (Martins and Aguas 1999). Clearly, the pathogenesis of tuberculosis in NOD mice is a complex process and requires further clarification.

A rat model of type1 diabetes was eventually developed in 1998 in Japan, and was named the Komeda diabetes-prone (KDP) rat (Komeda et al. 1998; Yokoi et al. 2003). It is reported that Cb1b, a member of the Cbl/Sli family of ubiquitin-protein ligases, is a major susceptibility gene for rat type 1 diabetes mellitus (Yokoi et al. 2002). This research background led us to re-examine the pathophysiology of pulmonary tuberculosis in type 1 diabetic rats. Our results suggest that type 1 diabetic rats are more susceptible to *M. tuberculosis* infection than non-diabetic rats.

Materials and Methods

Animals

Six-week-old female type 1 diabetic rats and sex- and age-matched control Long-Evans Tokushima lean (LETL) rats were purchased from SLC Co. (Shizuoka, Japan) (Komeda et al. 1998). The diabetic rats are not obese and develop insulitis with lymphocyte infiltration over time, being responsive to rabbit insulin, which ameliorates the diabetes. Hyperlipidemia and hypercholesterolemia are not recognized in KDP rats. The blood glucose level in this model was measured with an Ascensia Brio blood glucose measurement apparatus (Bayer Medical Co., Tokyo, Japan) with a measurement range of 30-550 mg/dl. All rats were housed in a biosafety level 3 facility and given rat chow and water *ad libitum* after aerosol infection with *M. tuberculosis* Kurono strain. The degree of severity of type 1 DM in the diabetic rats was evaluated mainly by assessment of blood glucose levels. Blood glucose levels in the rats were between 200 and 550 mg/dl.

Experimental infections

The Kurono strain of *M. tuberculosis* (ATCC35812) was grown in Middlebrook 7H9 broth for two weeks, and then filtered with a sterile acrodisc syringe filter with a pore size of 5.0 μm. Aliquots of the bacterial filtrate were stored at −80°C until use. The diabetic and WT rats were infected via the airborne route by placing them in an exposure chamber in a Glas-Col aerosol generator (Glas-Col, Inc., Terre Haute, IN, USA) (Sugawara et al. 2004). The nebulizer compartment was filled with 5 ml of a suspension containing 3×10^6 colony-forming units (cfu) of Kurono tubercle bacilli so that approximately 200 bacteria would potentially be deposited in the lungs of each animal. Inhalation infection experiments were carried out twice.

For some experiments, the diabetic rats were treated with 100 μl rabbit insulin (10 ng/ml, Shibayagi Co., Takasaki, Gunma, Japan) twice daily from the day after aerosol infection. The blood glucose level of the insulin-treated KDP rats was less than 200 mg/dl. Permission to perform the experiments on the animals was granted by the Animal Experiment Committee at the Research Institute of Tuberculosis.

Colony-forming unit (cfu) assay

At 7 weeks after aerosol infection, the rats were anesthetized with pentobarbital sodium. The right lobe of each lung and part of the spleen tissue were weighed and used to evaluate the *in vivo* growth of mycobacteria. The lung and spleen tissues were homogenized with a mortar and pestle, and 1 ml of a sterile dilution of the homogenate was cultured on 1% Ogawa egg medium. Colonies were counted after four weeks of incubation at 37°C (Yamada et al. 2001).

In vitro effect of glucose on mycobacterial growth

Diabetes is characterized by hyperglycemia. In order to examine the *in vitro* effect of glucose on *M. tuberculosis* growth, 0.1%, 0.5% and 1% glucose (w/v) was added to *M. tuberculosis* Kurono strain in 7H9 medium and the mixture was cultured for one week. Thereafter, the 10-fold-diluted culture suspension was cultured on 1% Ogawa egg medium for four weeks and the colonies

were counted.

Histopathology

For light microscopy, the rats were sacrificed seven weeks after infection. Tissue sections were cut from paraffin blocks containing lung, liver or spleen tissue and stained with hematoxylin and eosin or by the Ziehl-Neelsen method for acid-fast bacilli (Sugawara et al. 2004).

Real-time PCR

Another portion of the remaining right lower lobes of the lungs was used for reverse transcriptase PCR (RT-PCR) analysis to examine the expression levels of several cytokine mRNAs in these samples during *M. tuberculosis* infection. These samples were snap-frozen in liquid nitrogen and stored at −85°C until use. RNA extraction was performed as described previously (Yamada et al. 2005). Briefly, the frozen tissues were homogenized in a microcentrifuge tube with an autoclaved disposable 1000-μL tip cooled by dipping in liquid nitrogen. Then the homogenates were treated with 1 mL of TRIzol reagent (Invitrogen Japan Co., Tokyo, Japan), as specified by the manufacturer. After RNA isolation, total RNA concentration was measured with a spectrophotometer, and the agarose gel electrophoresis pattern of the total RNA was examined. The total RNAs were reverse-transcribed into cDNA with Moloney murine leukemia virus reverse transcriptase (Invitrogen). ABI Taqman® Gene Expression Assay was used for relative quantitative measurement of the mRNA expression of interferon (IFN)-γ, tumor necrosis factor (TNF)-α, and interleukin (IL)-1β (Yamada et al. 2005). A TaqMan® Rodent GAPDH Control Reagents set was used for normalization for data analysis. Real-time RT-PCR was performed according to the instructions for the ABI PRISM 7900HT Sequence Detection System (Applied BioSystems Inc.). Data were analyzed by the $\Delta\Delta C_T$ method using the ABI PRISM Sequence Detection System software package (version 2.1; Applied BioSystems, California, USA) running on Windows 2000. The results obtained from diabetic and control rats were expressed as relative expression quantities of the targets in comparison with those of non-infected rats that were calibrated with the expression of an internal control gene glyaraldehyde-3-phosphate dehydrogenase (GAPDH) (Yamada et al. 2005; Yamada et al. 2007).

Alveolar macrophage nitric oxide (NO) assay

Alveolar macrophages (3×10^5/well) were plated in 96-well culture plates in RPMI 1640 (Sigma-Aldridge, St. Louis, MO, USA) supplemented with 10% heat-inactivated fetal calf serum and then stimulated with *M. tuberculosis* Kurono strain and cultured overnight. The supernatants were collected 16 hours after culture seeding, filtered, and their NO concentrations were determined by the Griess assay as described previously (Green et al. 1990; Sugawara et al. 2004).

Statistical analysis

All values were expressed as means±S.E. and compared using Student's t test. For all statistical analyses, the level of statistical significance was set at $p < 0.01$.

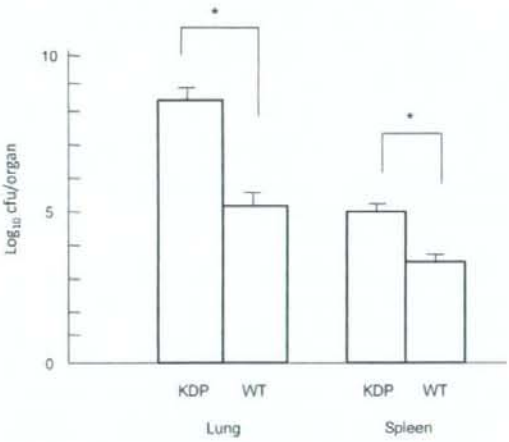

Fig. 1. Mycobacterial burden in the lung and spleen tissue of type 1 diabetic rats.
Colony-forming units (cfu) in lung and spleen tissues from type 1 diabetic (KDP) rats and wild-type rats exposed to 3×10^6 cfu of *M. tuberculosis* Kurono strain by aerosol infection. Seven weeks after infection, three rats from each group were sacrificed, and homogenates of the lungs and spleen were cultured. There is a significant difference in the lung and spleen cfu counts between KDP and WT rats ($p < 0.01$).
Error bars indicate standard deviation (SD) from the mean. *$p < 0.01$ vs. WT rats.

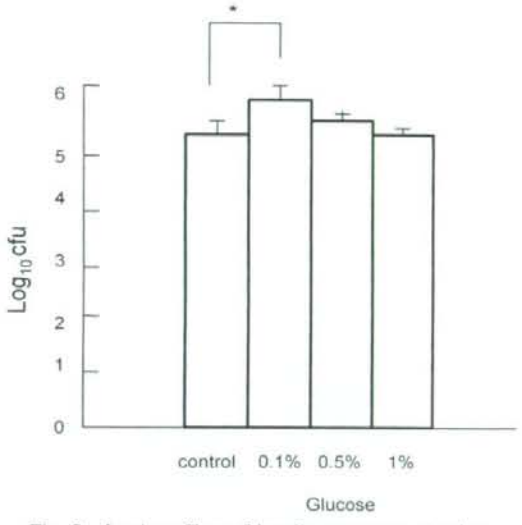

Fig. 2. *In vivo* effect of insulin treatment on tubercle bacilli in granulomas.
Type 1 diabetic (KDP) rats were treated with 100 μl rabbit insulin (10 ng/ml, Shibayagi Co., Takasaki, Gunma, Japan) twice daily from the day after aerosol infection. *$p < 0.01$ vs. WT rats.

Results

Mycobacterial burden in the lung and spleen tissue of KDP rats

When diabetic and WT LETL rats were infected via the airborne route with the Kurono strain of *M. tuberculosis* (3×10^6), all rats survived until the date of sacrifice (49 days after infection). As shown in Fig. 1, the number of mycobacterial colonies in the lung and spleen tissues increased, and there was a significant difference in the lung and spleen cfu counts between diabetic and WT rats ($p < 0.01$).

When insulin was administered to the diabetic rats subcutaneously twice daily, it reduced pulmonary and splenic cfu counts significantly ($p < 0.01$) and their cfu counts were similar to those in WT rats (Fig. 2).

Histopathology of infection

When 3×10^6 cfu of the Kurono strain was given to the rats via the airborne route, larger granulomas were recognized in the lungs of the diabetic rats than in the WT controls (Fig. 3A). No Langerhans-like multinucleated giant cells were found in the granulomatous lesions. No necrotic lesions were present in these granulomas. The pulmonary granulomas merged with the surrounding granulomas over time, and foamy epithelioid macrophages were more prominent. Although no tubercle bacilli were noted in the pulmonary granulomas of WT rats, acid-fast tubercle bacilli were more prominent in the granulomas of diabetic rats (Fig. 3B). Small granulomas were recognized in the spleen and liver of diabetic rats. Conversely, the granulomas of WT rats were discrete and isolated (Fig. 3C).

The diabetic rats, which were given insulin twice daily after infection, were dissected histologically. The sizes of pulmonary granulomas in the insulin-treated diabetic rats were found to be reduced significantly (Fig. 3D).

In vitro effect of glucose on mycobacterial growth

Three different concentrations of glucose were added to *M. tuberculosis* in 7H9 liquid medium. Mycobacterial growth was concentration-dependent (Fig. 4), and maximal when 0.1% glucose was added to the tubercle bacilli ($p < 0.01$). Although 0.5% glucose also increased mycobacterial growth, the difference between 0.5% glucose and no addition was not statistically significant. Addition of 1% glucose did not induce growth of tubercle bacilli significantly (Fig. 4).

Real-time PCR

The data thus obtained were expressed as relative intensity (Fig. 5). In the lung tissues of non-infected KDP and WT rats, the expression levels of IFN-γ, TNF-α and IL-1β mRNA were very low (< 0.1 as relative intensity). The expression of pulmonary IFN-γ mRNA was higher at 7 weeks after infection in the infected diabetic rats than in control rats, the mRNA expression in the former being > 3 times that in the latter ($p < 0.01$). Pulmonary TNF-α mRNA expression in the infected diabetic rats was 4 times higher than in the infected control rats ($p < 0.01$). On the other

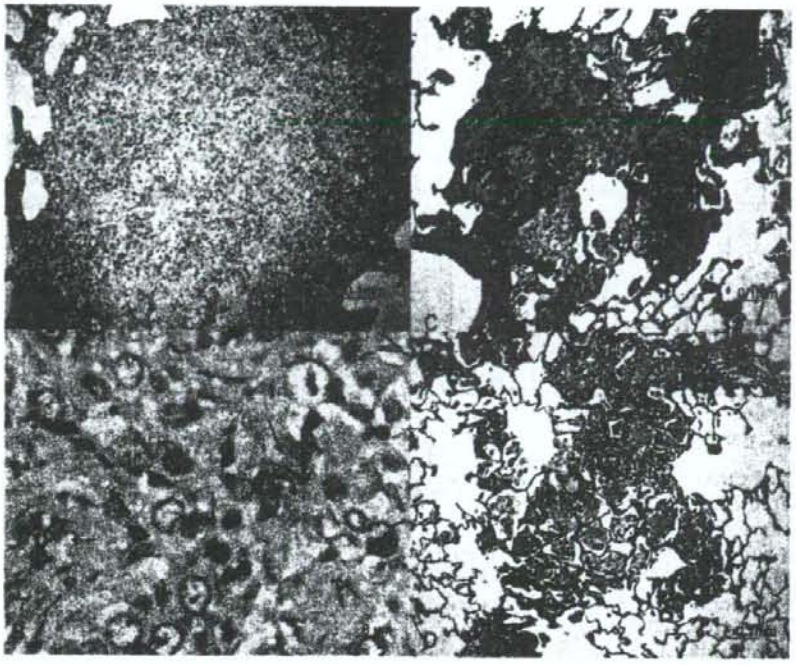

Fig. 3. Histopathology of the infected lung tissue.
Formalin-fixed sections were stained with hematoxylin and eosin (A, C and D) and Ziehl-Neelsen stain for acid-fast bacilli (→) (B).
(A) Pulmonary tissue from a diabetic type 1 (KDP) rat infected with the Kurono strain (7 weeks after infection)(magnification, × 100). (B) Pulmonary tissue from a KDP rat infected with the Kurono strain 7 weeks after infection (magnification, × 500) (C) Pulmonary tissue from a wild-type (WT) rat infected with the Kurono strain (7 weeks after infection)(magnification, × 100). (D) Pulmonary tissue from a KDP rat infected with the Kurono strain and treated with insulin twice daily (7 weeks after infection) (magnification, × 100). Larger granulomas were recognized in the lungs of KDP rats than in the WT controls (A). The sizes of pulmonary granulomas in the insulin-treated KDP rats were reduced significantly (D).

hand, the pattern of expression of pulmonary IL-1β mRNA was slightly different, and two times higher than in the infected controls.

Nitric oxide (NO) assay

NO levels in the culture supernatants of alveolar macrophages were determined using Griess reagent with reference to a standard $NaNO_2$ curve. The levels of NO produced by unstimulated alveolar macrophages from both KDP and WT rats were $< 20\,\mu$M. However, when the alveolar macrophages were stimulated overnight with the Kurono strain (multiplicity of infection=10), NO levels increased to $65 \pm 5\,\mu$M (control rats) and $25 \pm 2\,\mu$M (type 1 diabetic rats). The difference in NO secretion capacity between diabetic and WT rats was statistically significant ($p < 0.01$) (Table 1).

Discussion

In this study, large granulomas were induced in rats with type 1 diabetes after aerosol infection with *M. tuberculosis*. The number of cfu in lung and spleen tissues taken from the diabetic rats was significantly higher than that in WT control rats ($p < 0.01$). Similar findings were obtained when the experiments were repeated.

Although central necrosis was not recog-

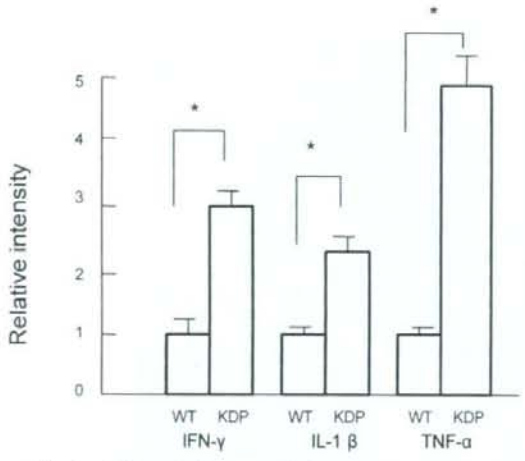

Fig. 4. Effect of glucose addition on *in vitro* mycobacterial growth.
$^*p < 0.01$ vs. WT rats. Glucose at 0.1%, 0.5% and 1% (w/v) was added to the *M. tuberculosis* Kurono strain in 7H9 medium, and the mixture was cultured for one week. Four weeks later, the number of cfu was determined.

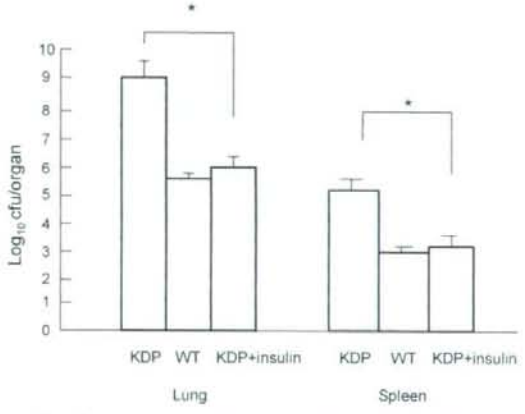

Fig. 5. *In vivo* expression profiles of pulmonary mRNA for IFN-γ, TNF-α or IL-1β in Kurono strain-infected rats. $^*p < 0.01$ vs. WT rats.
KDP, diabetic type 1; WT, wild-type. Pulmonary IFN-γ and TNF-α mRNA expression in the infected diabetic rats was significantly higher than in the infected control rats ($p < 0.01$)

TABLE 1. Nitric oxide (NO) production by alveolar macrophages stimulated with *M. tuberculosis* Kurono strain overnight.

Rat	Amount of NO produced (μM)	
	Unstimulated	Stimulated with Kurono strain
KDP	< 20	25 ± 2
WT	< 20	65 ± 5*

Alveolar macrophages (1×10^6/well) were plated in 96-well microculture plates in RPMI 1640 supplemented with 10% heat-inactivated fetal calf serum and stimulated with the Kurono strain overnight (multiplicity of infection=10). The NO concentration in the supernatants was determined by the Griess assay. Each value is mean±S.D. of the mean of three independent experiments. $^*p < 0.01$ vs. WT rats.

nized in the granulomas of diabetic rats, larger granulomas were induced in diabetic rats after infection with *M. tuberculosis*. Blood glucose levels ranged from 200 to 550 mg/dl. Impaired insulin secretion and hyperglycemia have been reported in diabetic rats (Komeda et al. 1998; Yokoi et al. 2003). As glucose induced mycobacterial growth significantly *in vitro*, a high glucose level in blood may be responsible for growth of *M. tuberculosis in vivo*. Impaired glucose tolerance may also be associated with active tuberculosis (Kimura et al. 1982; Oluboyo et al. 1990). The blood glucose level after *M. tuberculosis* infection did not increase significantly in diabetic and wild-type (WT) rats. Although clinical diabetes mellitus is frequently associated with hyperlipidemia and hypercholesterolemia (Powers 2008), blood lipid and cholesterol levels in diabetic rats were within the normal ranges. Hyperglycemia is common in patients with tuberculosis, and individuals who have no prior history of diabetes mellitus (DM) may present with glucose intolerance at the time of diagnosis. In a study of 506 patients with active pulmonary tuberculosis, nine had a history of DM, 25 were found to be newly diabetic, and 82 had impaired glucose tolerance (Mugusi et al. 1990). This suggests that, like other serious

infections, active tuberculosis is associated with hyperglycemia. Our laboratory findings have provided substantial evidence to support this clinical observation.

TNF-α, IFN-γ and IL-1β are important inflammatory cytokines. A few clinical studies have investigated serum cytokine levels in DM patients (Maltezos et al. 2002; Ozer et al. 2003). The highest serum IL-1α and IFN-γ levels were found in newly diagnosed type 1 DM patients without diabetic ketoacidosis. Expression of TNF-α, IFN-γ and IL-1β mRNA was relatively high at 7 weeks after infection, indicating that inflammatory changes in the lungs flare up, and may explain the large granulomas in type 1 diabetic rats.

Although no significant difference was noted in phagocytosis of tubercle bacilli by alveolar macrophages from diabetic type 1 and WT rats (data not shown), alveolar macrophages from the diabetic rats produced less NO than those from WT rats. NO is a well-known anti-tuberculous substance synthesized by inducible NO synthase in macrophages (Chan et al. 1992). Therefore, it is thought that alveolar macrophages from diabetic rats cannot be activated fully to produce NO upon stimulation with tubercle bacilli. Similar findings have been obtained in GK type 2 diabetic rats (Goto et al. 1976; Sugawara et al. 2004).

It is very important to measure the blood insulin level in diabetic rats because lack of insulin leads to hyperglycemia, which results in mycobacterial growth. When type 1 diabetic *M. tuberculosis*-infected rats were treated subcutaneously with insulin daily, the blood glucose level dropped from more than 550 mg/dl to ca. 200 mg/dl, and the number of cfu in the infected lung and spleen tissues was significantly decreased ($p < 0.01$). Thus, it is important to maintain the blood glucose level within the normal range to protect diabetic hosts from severe mycobacterial infection.

Diabetic type 1 rats are model animals of DM type 1. No studies have investigated the relationship between type 1 DM and mycobacterial infection using DM animal models. Non-obese diabetic (NOD) mice are a well-known model of type 1 DM and develop autoimmune diabetes, but there have been few studies of DM and mycobacterial infection. Diabetes-prone NOD mice are resistant to *M. avium* and the infection prevents autoimmune diabetes (Bras and Aguas 1996). In order to explain the mechanism of *M. avium*-induced resistance to insulin-dependent DM in NOD mice, the role of Fas and Th1 cells, and the increase in cytotoxicity of T cells have been highlighted (Martins and Aguas 1999). NOD mice are able to control *M. avium* infection, following a pattern similar to that observed in infected C3H mice. However, no report has indicated whether NOD mice can control *M. tuberculosis* infection. As the pathogenesis of DM in NOD mice is complicated, we chose the type 1 diabetic rat, a model established in 1998, to study the relationship between type 1 DM and tuberculosis. Unlike the findings observed in NOD mice, the diabetic rats displayed a different pattern in terms of histopathology and cfu count in lung and spleen tissues. Diabetic type 1 rats cannot control *M. tuberculosis* infection. Histopathology and cfu changes observed in the diabetic rats are similar to those in Goto Kakizaki (GK) rats. Much research has focused on diabetic type 1 rats in terms of the presence of insulin autoantibody, T cell function and islet cell antibody. We have already found that such rats have a high incidence of insulitis with lymphocyte infiltration and a good response to insulin treatment.

In conclusion, mycobacterial infection was studied in diabetic rats to investigate the basis for the high incidence of clinical tuberculosis in diabetic human patients. Our current findings clearly indicate that both GK type 2 diabetic and type 1 diabetic rats are highly susceptible to *M. tuberculosis* infection. Another important finding is that alveolar macrophages from KDP rats are not fully activated for killing of tubercle bacilli, unlike those from GK rats. Future studies should focus on the role of transcription factors in diabetic rats because NK-κB, STAT 4 and IRF-1 regulate the expression of interferons, IL-1 and TNF-α (Sugawara et al. 2003; Yamada et al. 2001; Yamada et al. 2002).

Acknowledgments

This study was supported in part by a Research Grant for Emerging and Re-emerging Infectious Diseases from the Ministry of Health, Welfare and Labour, Japan.

References

Banyai, A.L. (1931) Diabetes and pulmonary tuberculosis. *Am. Rev. Tuberc.*, **24**, 650-667.

Boucot, K.K., Dillon, E., Cooper, D. & Muer, P. (1952) Tuberculosis and diabetes. *Am. Rev. Tuberc.*, **65**, Suppl. 1, 1-50.

Bras, A. & Aguas, A.P. (1996) Diabetes-prone NOD mice are resistant to *Mycobacterium avium* and the infection prevents autoimmune disease. *Immunology*, **89**, 20-25.

Chan, J., Xing, Y., Magliozzo, R.S. & Bloom, B.R. (1992) Killing of virulent *Mycobacterium tuberculosis* by reactive nitrogen intermediates produced by activated murine macrophages. *J. Exp. Med.*, **175**, 1111-1122.

Garay, S.M. (2004) Pulmonary tuberculosis In Tuberculosis (ed. by Rom, W.N. and Garay, S.M.). p. 345. LWW, Philadelphia.

Goto, Y., Kakizaki, M. & Masaki, N. (1976) Production of spontaneous diabetic rats by repetition of selective breeding. *Tohoku J. Exp. Med.*, **119**, 85-90.

Green, S.J., Crawford, R.M., Hockmeyer, J.T., Meltzer, M.S. & Nacy, C.A. (1990) Leishmania major amastigotes initiate the L-arginine-dependent killing mechanism in IFN-γ stimulated macrophages by induction of tumor necrosis factor-α. *J. Immunol.*, **145**, 4290-4297.

Kim, S.J., Hong, Y.P., Lew, W.J., Yang, S.C. & Lee, E.G. (1995) Incidence of pulmonary tuberculosis among diabetics. *Tuber. Lung Dis.*, **76**, 529-533.

Kimura, K., Toyota, T., Kakizaki, M., Kudo, M., Takebe, K. & Goto, Y. (1982) Impaired insulin secretion in the spontaneous diabetic rats. *Tohoku J. Exp. Med.*, **137**, 453-459.

Komeda, K., Noda, M., Terao, K., Kuzuya, N., Kanazawa, M. & Kanazawa, Y. (1998) Establishment of two substrains, diabetes-prone and non-diabetic, from Long-Evans Tokushima lean (LETL) rats. *Endocr. J.*, **45**, 737-744.

Makino, S., Kunimoto, K., Muraoka, Y., Mizushima, Y., Katagiri, K. & Tochino, Y. (1976) Breeding of a non-obese, diabetic strain of mice. *Exp. Animals*, **29**, 1-13.

Maltezos, E., Papazoglou, D., Exiara, T., Papazoglou, L., Karathanasis, E., Christakidis, D. & Ktenidou-Kartali, S. (2002) Tumor necrosis factor-α levels in non-diabetic offspring of patients with type 2 diabetes mellitus. *J. Int. Med. Res.*, **30**, 576-583.

Martins, T.C. & Aguas, A.P. (1999) Mechanisms of *Mycobacterium avium*-induced resistance against insulin-dependent diabetes mellitus (IDDM) in non-obese diabetic (NOD) mice: role of Fas and Th1 cells. *Clin. Exp. Immunol.*, **115**, 248-254.

Mugusi, F., Swai, A.B.M., Alberti, K.G.M.M. & McLarty, D.G. (1990) Increased prevalence of diabetes mellitus in patients with pulmonary tuberculosis in Tanzania. *Tubercle*, **71**, 271-276.

Oluboyo, P.O. & Erasmus, R.T. (1990) The significance of glucose intolerance in pulmonary tuberculosis. *Tubercle*, **71**, 135-138.

Ozer, G., Teker, Z., Cetiner, S., Yilmaz, M., Topaloglu, A.K., Oneli-Mungan, N. & Yuksel, B. (2003) Serum IL-1, IL-2, TNF-α and IFN-γ levels of patients with type 1 diabetes mellitus and their siblings. *J. Pediatr. Endocrinol. Metab.*, **16**, 203-210.

Powers, A.C. (2008) Diabetes mellitus. In Harrison's principle of internal medicine (ed. by Fauci, A., Braunwald, E., Kasper, D., Hauser, S., Lomgo, D., Jameson, J. & Loscalzo, J.) p. 2275. McGraw-Hill, New York.

Root, H.F. (1934) The association of diabetes and tuberculosis. *N. Eng. J. Med.*, **210**, 1-13.

Sugawara, I., Yamada, H. & Mizuno, S. (2003) Relative importance of STAT 4 in murine tuberculosis. *J. Med. Microbiol.*, **52**, 29-34.

Sugawara, I., Yamada, H. & Mizuno, S. (2004) Pulmonary tuberculosis in spontaneously diabetic Goto Kakizaki rats. *Tohoku J. Exp. Med.*, **204**, 135-145.

Yamada, H., Mizuno, S., Reza-Gholizadeh, M. & Sugawara, I. (2001) Relative importance of NF-κB p50 in mycobacterial infection. *Infect. Immun.*, **69**, 7100-7105.

Yamada, H., Mizuno, S. & Sugawara, I. (2002) Interferon regulatory factor 1 in mycobacterial infection. *Microbiol. Immunol.*, **46**, 751-760.

Yamada, H., Udagawa, T., Mizuno, S., Hiramatsu, K. & Sugawara, I. (2005) Newly designed primer sets available for evaluating various cytokines and iNOS mRNA expression in guinea pig lung tissues by RT-PCR. *Exp. Anim.*, **54**, 163-172, 2005.

Yamada, H., Mizuno, S., Ross, A.C. & Sugawara, I. (2007) Retinoic acid therapy attenuates the severity of tuberculosis while altering lymphocyte and macrophage numbers and cytokine expression in rats infected with *Mycobacterium tuberculosis*. *J. Nutr.*, **137**, 2696-2700.

Yokoi, N., Komeda, K., Wang, H.Y., Yano, H., Kitada, K., Saitoh, Y., Seino, Y., Yasuda, K., Serikawa, T. & Seino, S. (2002) Cb1b is a major susceptibility gene for rat type 1 diabetes mellitus. *Nat. Genet.*, **31**, 391-394.

Yokoi, N., Namae, M., Fuse, M., Wang, H.Y., Hirata, T., Seino, S. & Komeda, K. (2003) Establishment and characterization of the Komeda diabetes-prone rat as a segregating inbred strain. *Exp. Anim.*, **52**, 295-301.

Clinical Immunology (2008) 128, 366–373

available at www.sciencedirect.com

ScienceDirect

www.elsevier.com/locate/yclim

Disruption of Nrf2 enhances susceptibility to airway inflammatory responses induced by low-dose diesel exhaust particles in mice

Ying Ji Li [a,d], Hajime Takizawa [b], Arata Azuma [c], Tadashi Kohyama [e], Yasuhiro Yamauchi [e], Satoru Takahashi [f], Masayuki Yamamoto [f], Tomoyuki Kawada [a], Shoji Kudoh [c], Isamu Sugawara [d,*]

[a] Department of Hygiene and Public Health, Nippon Medical School, Tokyo, Japan
[b] Fourth Department of Internal Medicine, Teikyo University, School of Medicine, Kawasaki, Japan
[c] Department of Pulmonary Medicine/Infection and Oncology, Nippon Medical School, Tokyo, Japan
[d] Mycobacterial Reference Center, The Research Institute of Tuberculosis, Kiyose, Japan
[e] Department of Respiratory Medicine, University of Tokyo, School of Medicine, Tokyo, Japan
[f] Institute of Basic Medical Sciences, University of Tsukuba, Ibaragi, Japan

Received 15 April 2008; accepted with revision 19 May 2008
Available online 9 July 2008

KEYWORDS
Nrf2;
Diesel exhaust particle;
Cytokine;
Airway hyperresponsiveness;
Eosinophils;
Mouse model

Abstract To test our hypothesis that diesel exhaust particle (DEP)-induced oxidative stress and host antioxidant responses play a key role in the development of DEP-induced airway inflammatory diseases, C57BL/6 nuclear erythroid 2 P45-related factor 2 (Nrf2) knockout ($Nrf2^{-/-}$) and wild-type mice were exposed to low-dose DEP for 7 h/day, 5 days/week, for 8 weeks. $Nrf2^{-/-}$ mice exposed to low-dose DEP showed significantly increased airway hyperresponsiveness and counts of lymphocytes and eosinophils, together with increased concentrations of IL-12 and IL-13, and thymus and activation-regulated chemokine (TARC), in BAL fluid than wild-type mice. In contrast, expression of antioxidant enzyme genes was significantly higher in wild-type mice than in $Nrf2^{-/-}$ mice. We have first demonstrated that disruption of Nrf2 enhances susceptibility to airway inflammatory responses induced by inhalation of low-dose DEP in mice. These results strongly suggest that DEP-induced oxidative stress and host antioxidant responses play some role in the development of DEP-induced airway inflammation.

Introduction

Air pollution is associated with increased mortality and morbidity. Although air pollutants include both gaseous components (ozone, carbon monoxide, sulfur dioxide, and nitrogen dioxide) and particulate components, it has been shown that particulates, particularly PM10 (particulate matter with diameter less than 10 μm), are more relevant to many disorders. Currently, much attention is being focused on PM2.5 in relation to adverse health effects. Diesel exhaust particles (DEP) are the major component of PM2.5, and therefore the relationship between PM2.5 or PM10 and some diseases has been investigated

* Corresponding author. Fax: +81 424 92 4600.
E-mail address: sugawara@jata.or.jp (I. Sugawara).

1521-6616/$ – see front matter © 2008 Elsevier Inc. All rights reserved.
doi:10.1016/j.clim.2008.05.005

intensively [1–5]. The roles of reactive oxygen species (ROS) generated by exposure to DEP and the subsequent generation of the oxidative stress response have been emphasized through *in vitro* experimental studies [6–11]. These findings suggest that DEP induce activation of transcription factors and that ROS may play an important role in these processes. Thus, imbalance between oxygen stress/proinflammatory proteins and antioxidant proteins may be a key player in the development of hazardous effects. However, it is still not fully clear whether oxidative stress caused by inhalation of DEP leads to airway inflammation and airway hyperresponsiveness *in vivo*.

We have shown previously that continuous low-level exposure to DEP (100 $\mu g/m^3$ for 7 h/day, 5 days/week) significantly augments AHR and Th2-type cytokine/chemokine gene expression in murine asthma models [12]. Studies using two different mouse strains have demonstrated a difference in susceptibility to DEP exposure between them, and suggested that certain antioxidant enzymes may play an important role in susceptibility, C57BL/6 mice being more sensitive to low-dose DEP exposure than BALB/c mice [13,14].

Nuclear erythroid 2 P45-related factor 2 (Nrf2) is a redox-sensitive basic leucine zipper transcription factor that is involved in the transcriptional regulation of many antioxidant genes. The Nrf2-regulated genes in the lungs include almost all of the relevant antioxidant enzymes, such as HO-1 and several members of the GST family [15]. Therefore, to clarify whether or not oxidative stress and host antioxidant defenses play a central role in the pathogenesis of lung disease, several disease models using Nrf2 $^{-/-}$ mice have been studied, including ovalbumin (OVA)-induced asthma [16], bleomycin-induced lung fibrosis [17], and cigarette smoke-induced emphysema [18]. It is reported that oxidative stress is involved in the development of DEP-induced airway inflammation [6–11] and that Nrf2 is also a key transcription factor that regulates antioxidant and defense action against the proinflammatory and oxidizing effects of DEP *in vitro* [9,11]. Furthermore, DNA adduct formation has been shown to be accelerated in the lungs of Nrf2 $^{-/-}$ mice exposed to DEP (3 mg/m^3 for 4 weeks) [19]. However, no study has yet utilized Nrf2 $^{-/-}$ mice to examine the pathogenesis of airway inflammation induced by low-dose DEP.

To test the hypothesis that DEP-induced oxidative stress and host antioxidant responses play a key role in the development of DEP-induced airway inflammatory disease *in vivo*, we conducted the present study using C57BL/6 Nrf2 $^{-/-}$ and Nrf2$^{+/+}$ mice, and examined airway inflammatory responses and host antioxidant responses to low-dose DEP (i.e., at concentrations similar to those inhaled outdoors) exposure.

Materials and methods

Animals

Nrf2-deficient C57BL/6 mice were generated as described by Itoh et al. [20]. Mice were genotyped for Nrf2 status by PCR amplification of genomic DNA extracted from the tail [21]. PCR amplification was performed using three different primers:

Nrf2-sense for both genotypes: 5′-TGGACGGGACTATTGAAGGCTG-3′
Nrf2-antisense for wild-type mice: 5′-GCCGCCTTTTCAGTAGATGGAGG-3′
Nrf2-antisense for LacZ: 5′-GCGGATTGACCGTAATGGGATAGG-3′.

Amplification was performed using 30 cycles of 96 °C 20 s, 59 °C 30 s, and 72 °C 45 s. The wild-type allele produces a 734-bp band, while the knockout allele produces a 449-bp band. Mice were housed under specific pathogen-free (SPF) conditions with controlled temperature and lighting (23±2 °C, 12 h light/dark periods). Age-matched 6-week-old female mice from the same litter were placed into chambers under same controlled conditions and exposed to DEP. All procedures conformed to the National Institutes of Health (NIH) guidelines for the care and use of laboratory animals.

DEP exposure

The *in vivo* DEP exposure system has been described previously [22,23]. The concentration of DEP was monitored and kept low (approximately 100 $\mu g/m^3$). C57BL/6 Nrf2 $^{-/-}$ and Nrf2$^{+/+}$ mice were exposed to DEP for 7 h daily, 5 days a week.

Experimental protocol

Nrf2 $^{-/-}$ and Nrf2$^{+/+}$ C57BL/6 mice were exposed to low-dose DEP or clean air (SPF) for 8 weeks. AHR was measured in all experimental groups immediately, and mice were sacrificed on day 56 of exposure to DEP or clean air in all experimental groups. We examined the histopathology of the lung tissues and the cell populations in BAL fluid. We also measured the concentrations of inflammatory cytokines and chemokines in the BAL fluid and the IgE, IgG_1 and IgG_{2a} levels in the serum. We also examined the gene expression of antioxidants in the lung tissues.

Determination of AHR

Airway hyperresponsiveness was assessed by whole-body plethysmography with a free-moving application (Buxco Electronics, Troy, NY) [24] in accordance with a previously published procedure [12,13].

Histological analysis

For histologic examination, 10% formalin-fixed lung tissues were embedded in paraffin, cut into sections, and stained with hematoxylin and eosin (HE), and periodic acid-Schiff (PAS). Histopathological changes were examined using a light microscope (Eclipse E800, Nikon, Tokyo, Japan).

BAL and cell differentials in BAL fluid

BAL was performed as described previously [13,14], and the total number of cells in the BAL fluid was counted with a hemocytometer. For differential counts of leukocytes in BAL fluid, cytospin smear slides (Lab Systems; Tokyo, Japan) were prepared and stained with Diff-Quick Romanowski stain (Muto Kagaku Co., Tokyo, Japan).

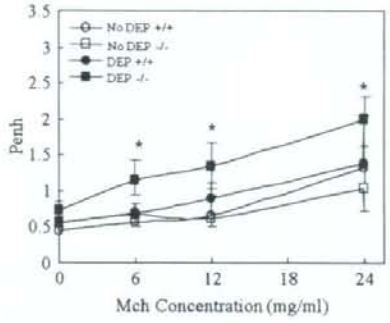

Figure 1 Airway hyperresponsiveness was assessed by whole-body plethysmography with free-moving application and then evaluated by Penh values in response to inhaled aerosolized methacholine (0, 6, 12, 24 mg/ml). The *X* axis shows the concentration of methacholine (mg/ml); the *Y* axis shows the values of Penh. $^{+/+}$, wild-type mice; $^{-/-}$, Nrf2 knockout mice. Results are means ± SD of data in each group ($n=16$). *$p<0.05$ $Nrf2^{-/-}$ mice vs $Nrf2^{+/+}$ mice at each methacholine concentration point.

Measurement of cytokines/chemokines in BAL fluid

Immunoreactivity for IL-12, IL-4, IL-13, MCP-1, eotaxin, RANTES, and TARC in the BAL fluid supernatants was measured with an enzyme-linked immunosorbent assay (ELISA) kit (Biosource International, Inc., Camarillo, CA). ELISA was carried out in accordance with the manufacturer's instruction sheet. Each sample was assayed in triplicate.

Measurement of IgG_1, IgG_{2a}, and IgE in serum

Immunoreactivity for IgG_1, IgG_{2a} (Cygnus Technologies, Inc., Southport, NC), and IgE (Bethyl Laboratories, Inc., Montgomery, TX) in the serum was measured with an ELISA kit in accordance with the manufacturer's instruction sheet. Each sample was assayed in triplicate.

Quantitative real-time reverse transcription-polymerase chain reaction (RT-PCR)

Total RNA was extracted from the lung tissues with TRIzol Reagent (Gibco BRL, Gaithersburg, MD) in accordance with the manufacturer's instructions. Complementary DNA (cDNA) was synthesized as described previously [25] and quantified with a sequence detector (7900HT Sequence Detection System; Applied Biosystems) using PCR Master Mix and the respective inventoried primers including a β-actin control (TaqMan Universal PCR Master Mix, Applied Biosystems). TaqMan assays were repeated in triplicate samples for each of the selected antioxidant enzyme genes in each lung sample. The mRNA expression levels for all samples were normalized to the level of the housekeeping gene β-actin. Selected antioxidant enzyme genes and their assay ID were as follows: glutamate-cysteine ligase, modifier subunit (GCLm, Mm00514996_m1), glutamate-cysteine ligase, catalytic subunit (GCLc, Mm00802655_m1), glucose-6-phosphate dehydrogenase X-linked (G6PD, Mm00656735_g1), glutathione-S-transferase, alpha3 (GST-α3, Mm00494798_m1), glutathione-S-transferase m1 (GST-M1, Mm00833915_g1), glutathione-S-transferase pi2 (GST-P2, Mm00839138_g1), heme-oxygenase-1 (HO-1, Mm00516004_m1), superoxide dismutase 2 (SOD2, Mm00449726_m1), glutathione reductase 1 (GSr, Mm00833903_m1), and β-actin (Mm00607939_s1).

Statistical analysis

Results are shown as means ± standard deviation (SD). Differences between groups were determined by Student's *t* test using the Stat Mate III software package (ATMS Digitals Medical Station, Tokyo, Japan). Differences at $p<0.05$ were considered significant.

Results

Assessment of changes in AHR in response to DEP exposure

To examine airway responses to low-dose DEP in $Nrf2^{-/-}$ mice, we first assessed AHR (as expressed in Penh) using whole-body plethysmography.

Exposure to DEP significantly increased the airway reactivity to methacholine (6, 12, and 24 mg/ml) in $Nrf2^{-/-}$ mice compared with $Nrf2^{+/+}$ mice (Fig. 1).

Lung histopathology

The histological specimens revealed no change in response to DEP exposure in $Nrf2^{+/+}$ mice (Fig. 2), but PAS staining-positive mucus cell hyperplasia was evident in $Nrf2^{-/-}$ mice (Fig. 2B). There were no inflammatory cell infiltrates in either $Nrf2^{+/+}$ or $Nrf2^{-/-}$ mice.

BAL cell differentials

Examination of the BAL fluid showed that the total number of cells and the number of macrophages were significantly lower in $Nrf2^{-/-}$ mice than in $Nrf2^{+/+}$ mice. The numbers of lymphocytes and eosinophils in the BAL fluid after DEP exposure were significantly higher in $Nrf2^{-/-}$ mice than in $Nrf2^{+/+}$ mice (Fig. 3).

Cytokine/chemokine levels in BAL fluid

The levels of IL-12 and IL-13 in BAL fluid after DEP exposure were significantly higher in $Nrf2^{-/-}$ mice. The level of IL-4 in BAL fluid did not change significantly after DEP exposure in either $Nrf2^{+/+}$ or $Nrf2^{-/-}$ mice (Fig. 4A). The level of TARC in BAL fluid after DEP exposure was significantly greater in $Nrf2^{-/-}$ mice than in $Nrf2^{+/+}$ mice. The levels of monocyte chemoattractant protein (MCP)-1, regulated upon activation, normal T expressed and secreted (RANTES) and Eotaxin in tBAL fluid were not changed significantly after DEP exposure in either $Nrf2^{+/+}$ or $Nrf2^{-/-}$ mice (Fig. 4B).

IgG_1, IgG_{2a}, and IgE levels in serum

There were no significant changes in the levels of IgE, IgG_1 and IgG_{2a} in serum after DEP exposure in either $Nrf2^{+/+}$ or $Nrf2^{-/-}$ mice (Fig. 5).

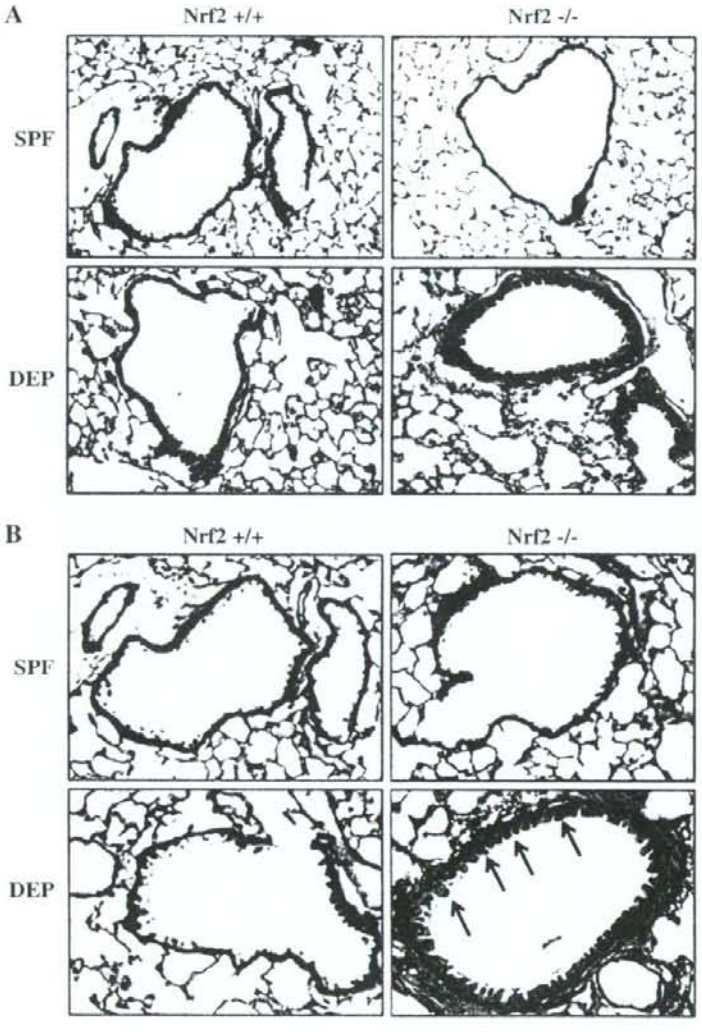

Figure 2 Histopathology of the lung tissues. Lung sections stained with HE and examined by light microscopy (100×) (A). Lung sections stained with PAS and examined by light microscopy (200×) (B). The arrows indicate the PAS-positive cells.

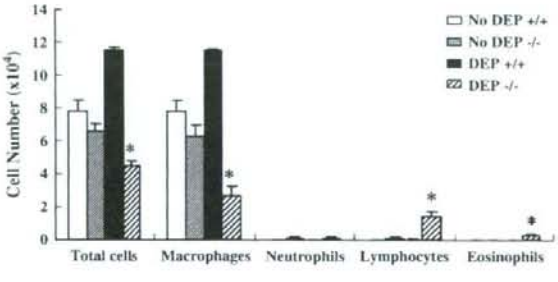

Figure 3 Changes in total cells and differentials in BAL fluid. The smear preparations in BAL fluid were stained with Diff-Quick Romanowski stain. Results are means ± SD of data in each group ($n=6$). *$p<0.05$ $Nrf2^{-/-}$ mice vs $Nrf2^{+/+}$ mice.

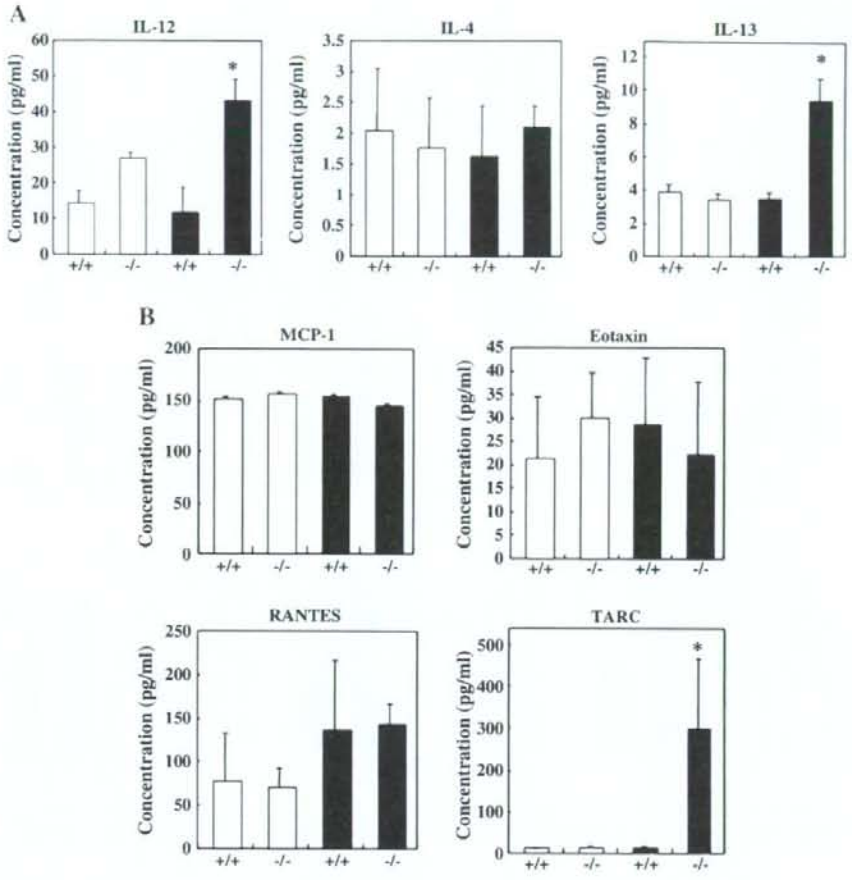

Figure 4 Cytokine (A) and chemokine (B) levels in BAL fluid as evaluated by ELISA. Clear bar, no DEP (not exposed to DEP) group; solid bar, DEP group; $^{+/+}$, wild-type mice; $^{-/-}$, Nrf2 knockout mice. Results are means ± SD of data in each group ($n=6$). *$p<0.05$ $Nrf2^{-/-}$ mice vs $Nrf2^{+/+}$ mice.

Induction of antioxidant enzyme genes in lung tissues

Changes in the expression of mRNA for various antioxidant enzymes were determined by real RT-PCR. After DEP exposure, the respective fold changes in mRNA expression in the lungs of $Nrf2^{+/+}$ and $Nrf2^{-/-}$ mice were: GCLm (3.4 vs 1.8), GCLc (5.5 vs 2.1), G6PD (18 vs 7.8), GST-α3 (7.4 vs 1.6), GST-M1 (6.2 vs 1.3), GST-P2 (6.4 vs 2.1), HO-1 (11.8 vs 6.9), SOD2 (17 vs 9.1), and GSr (8.8 vs 5.9) (Fig. 6). Thus, gene

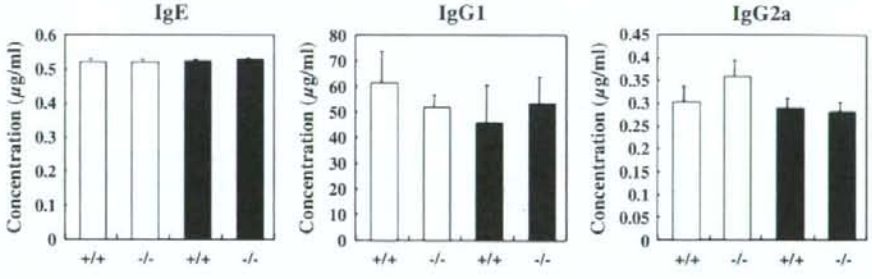

Figure 5 Immunoglobulin levels in sera evaluated by ELISA. Clear bar, no DEP (not exposed to DEP) group; solid bar, DEP group; $^{+/+}$, wild-type mice; $^{-/-}$, Nrf2 knockout mice. Results are means ± SD of data in each group ($n=6$).

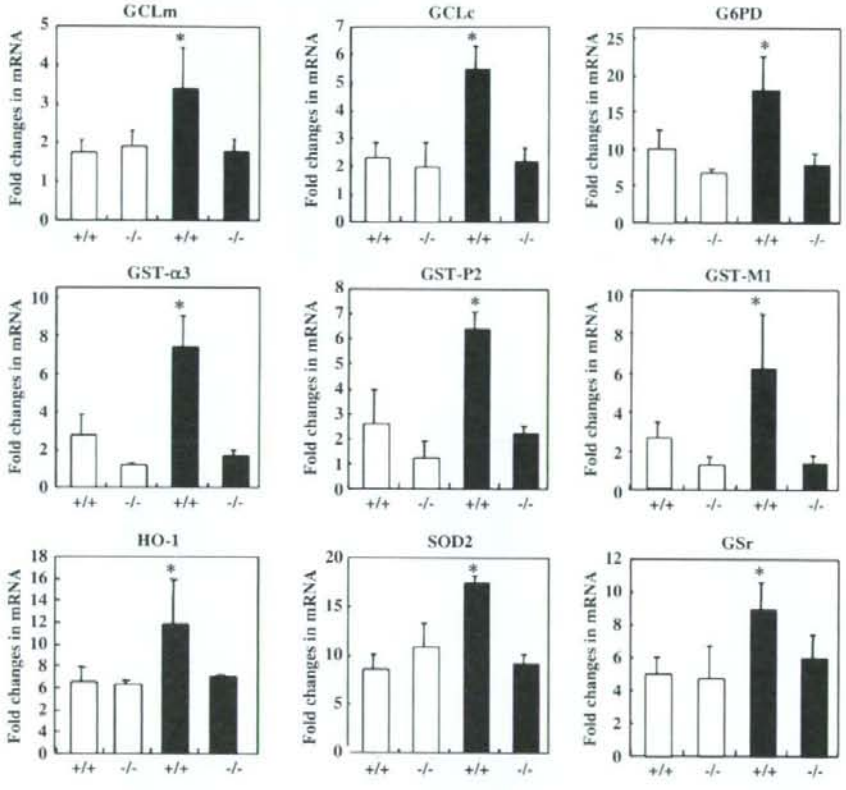

Figure 6 Real-time RT-PCR for genes of various antioxidants in the lungs. Clear bar, no DEP (not exposed to DEP) group; solid bar, DEP group; $^{+/+}$, wild-type mice; $^{-/-}$, Nrf2 knockout mice. Results are means ± SD of data in each group ($n = 3$). *$p < 0.05$ $Nrf2^{-/-}$ mice vs $Nrf2^{+/+}$ mice.

expression of various antioxidant enzymes was significantly increased in $Nrf2^{+/+}$ mice compared with $Nrf2^{-/-}$ mice.

Discussion

The present study using Nrf2 gene knockout mice revealed for the first time that disruption of the Nrf2 gene enhanced susceptibility to airway inflammatory responses induced by inhalation of low-dose DEP. $Nrf2^{-/-}$ and $Nrf2^{+/+}$ C57BL/6 mice were exposed to low-dose DEP (i.e., at concentrations similar to those inhaled outdoors) for 8 weeks, and in $Nrf2^{-/-}$ mice significant increases of AHR, numbers of lymphocytes and eosinophils, and levels of IL-12, IL-13 and TARC in BAL fluid were observed in comparison with those of $Nrf2^{+/+}$ mice. In contrast, gene expression of antioxidant enzymes was significantly increased in $Nrf2^{+/+}$ mice in comparison with $Nrf2^{-/-}$ mice. As the magnitude of gene induction of these antioxidant enzymes was considerably higher in $Nrf2^{+/+}$ than in $Nrf2^{-/-}$ mice, it was clearly associated with the activation of Nrf2 in response to DEP-induced lung inflammation.

We assessed airway hyperresponsiveness (as expressed by enhanced Pause values (Penh)) by whole-body plethysmography. Penh has been used in an experimental mouse model to evaluate airway hyperresponsiveness [26–28]. Exposure to DEP increased airway reactivity to methacholine more significantly in $Nrf2^{-/-}$ mice than in $Nrf2^{+/+}$ mice. Our previous study showed that the changes in Penh induced by methacholine were significantly greater 1 week after DEP exposure in C57BL/6 mice, but that Penh recovered to the baseline level by 8 weeks after DEP exposure, and the changes in AHR were independent of the airway inflammation caused by oxidative stress derived from low-dose DEP exposure [13]. The current data suggest that AHR may increase with oxidative stress induced by continuous, long-term (longer than 8 weeks) exposure to DEP in wild-type mice. PAS-positive mucus cell hyperplasia was found only in $Nrf2^{-/-}$ mice, without destruction of the airway epithelial cells in the lung tissues. Although it has been confirmed that AHR increases with oxidative stress induced by DEP exposure, the mechanism by which AHR increases in $Nrf2^{-/-}$ mice is still unclear. It is speculated that, in this system, the changes in AHR caused by low-dose DEP may depend on the genetic strain of mouse employed, as reported by Depuydt et al. [29]. Our results suggest that Nrf2 plays a key role in regulation of AHR in oxidative stress caused by DEP exposure.